Enhanced THz Radiation from Spatially Inhomogeneous Fields

Guang-Rui Jia(贾光瑞)[1,2], Deng-Xin Zhao(赵登欣)[1,3], Song-Song Zhang(张松松)[2], Zi-Wei Yue(岳梓巍)[2], Chao-Chao Qin(秦朝朝)[1], Zhao-Yong Jiao(焦照勇)[1], and Xue-Bin Bian(卞学滨)[1,3*]

[1]*School of Physics, Henan Normal University, Xinxiang 453007, China*
[2]*School of Materials Science and Engneering, Henan Normal University, Xinxiang 453007, China*
[3]*Wuhan Institute of Physics and Mathematics, Innovation Academy for Precision Measurement Science and Technology, Chinese Academy of Sciences, Wuhan 430071, China*

(Received 22 July 2023; accepted manuscript online 31 August 2023)

Nonlinear terahertz (THz) radiation from gas media usually relies on the asymmetric laser-induced current produced by ultra-intense two-color laser fields with a specific phase delay. Here a new scheme is proposed and theoretically investigated, in which the radiation is generated by spatially inhomogeneous fields induced by relatively low-intensity monochromatic lasers and an array of single triangular metallic nanostructures. Our simulations are based on the classical photocurrent model and the time-dependent Schrödinger equations separately. It is found that the collective motion of the ionized electrons can be efficiently controlled by the inhomogeneous field, resulting in strong residual currents. The intensity of the THz radiation could be enhanced by about two orders of magnitude by increasing the spatial inhomogeneity of the field.

DOI: 10.1088/0256-307X/40/10/103202

Owning to the excellent characteristics of ultrashort pulses in the terahertz (THz) range, they have been used in many aspects,[1–3] such as medical imaging, broadband communication, and security detection. Due to the huge application prospect of THz radiations,[4,5] research of intense THz pulse generation has received increasing attention. Since the ultrafast lasers provide reliable and stable driving sources, the THz radiation based on the tabletop lasers has developed rapidly.[6] So far, there have been several main techniques to generate intense THz waves. One of the methods is the optical rectification in nonlinear crystals, 10 MW/cm^2 THz pulse with conversion efficiency of 45% has been reported.[7] However, the material damage is still a notable issue for the further improvement. Another well-known method is based on the two-color laser mixing scheme.[8–12] An intense femtosecond pulse together with its second harmonic pulse are focused into a gas medium to ionize the atoms and molecules nonsymmetrically. Then the laser-induced plasma generates a transient current and produces intense broadband THz emissions.[13] This photocurrent model was proposed by Kim *et al.*[10–12,14] However, this conversion process requires high-intensity pulses (greater than 10^{14} W/cm^2), which are not directly attainable using a femtosecond oscillator. It also requires a precise control of the phase difference between the fundamental field and its second harmonic. A new simple THz generation scheme with high efficiency but requiring a relatively modest energy source pulse is in demand.

Recently, with the tremendous advance in nanoscale material engineering and manipulation techniques, a new emerging field called atto-nanophysics[15,16] appeared. Bulk samples have been scaled in size to nanometers, providing the probability of studying light-nanostructure interactions. For instance, a bow-tie shaped nanostructure fabricated on a sapphire plate has been designed to produce enhanced extreme-ultraviolet light.[17,18] With a modest laser pulse (only 10^{12} W/cm^2) focused onto the nanostructure, the enhancement factor exceeds 20 dB. Moreover, the extension of harmonic cutoff energy in inhomogeneous fields induced by the nanostructure has also been explored.[19–24] The extended cutoff feature was interpreted as the substantial modification of the electron trajectories and the confinement of the electron dynamics induced by the inhomogeneous fields. Furthermore, controlling the light-induced electron emission from nanotips and nanotapers paves the way for the nanoscale manipulation of electron dynamics.[25–28] The development of this field opens a new vision for the study of the ultrafast electron dynamics. It also increases the possibility for generating enhanced THz radiations with nanostructures.[29] However, to our knowledge, it has not been investigated theoretically or experimentally for the THz generation in gas media exposed to the inhomogeneous fields.

In this work, an array of metallic structures are exploited to interact with a relatively low intensity monochromatic laser pulse to generate a spatial inhomogeneous field. The spatial inhomogeneity is well described by the linear fitting method. Atoms in this field are driven to emit THz waves.[30] The effective field is enhanced by means of the nanostructure, which makes the tunneling ionization of atoms become dominant, some of the results has been confirmed by experiment.[17] At the same time, the spatial inhomogeneity will cause the asymmetric movement of the freed electrons, resulting in non-vanishing directional currents. With the increase of the inhomogeneity, the residual current shows an increasing trend, which leads to the enhancement of THz radiations.

Theoretical Methods. The classical transient plasma

*Corresponding author. Email: xuebin.bian@wipm.ac.cn
© 2023 Chinese Physical Society and IOP Publishing Ltd

current model can well explain the mechanism of the emission of phase-dependent THz waves in homogeneous fields. This model mainly includes the first two steps in the recollision model:[31] Firstly, the coulomb barrier is suppressed by the external laser field, the bound electrons tunnel through the barrier to the continuum states. Secondly, the freed electrons driven by the laser field can be seen as a classical particle by neglecting the Coulomb potential, whose trajectory can be obtained from Newton's equation. They can collectively form a directional current in the two-color fields, leading to the emission of THz waves.

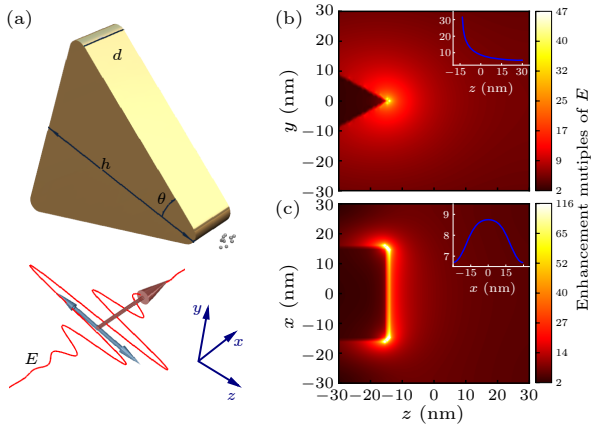

Fig. 1. Finite difference time domain simulations of the induced local electric field enhancement: (a) geometry of the single triangular metallic nanostructure, [(b), (c)] the enhancement multiples of local electric amplitude computed in both the y–z and x–z planes. The solid blue curves in (b) and (c) show the electric enhancement along both the z and x axes, respectively.

Here we extend the transient plasma current model to study the THz generation mechanism in inhomogeneity fields. As shown in Fig. 1(a), we exploit a single triangular metallic structure scaled in nanometers to enable the enhancement of laser field and the generation of spatial inhomogeneity. The shape can be characterized by three parameters: the altitude h, thickness d, and angle θ. For a given geometry of the nanostructure, the induced inhomogeneous field around its tip can be derived by finite difference time domain (FDTD) simulations.[32] In our simulations, we set $h = 300\,\text{nm}$, $d = 30\,\text{nm}$, $\theta = 30^\circ$. The focused laser intensity is $I = 3.9 \times 10^{12}\,\text{W/cm}^2$ at $\lambda = 800\,\text{nm}$. Figures 1(b) and 1(c) plot the distributions of the induced electric fields in the x–z and y–z planes. One can see that the enhancement of the electric field demonstrates a strong spatial inhomogeneity around the tip of the nanostructure.

With a relatively modest laser pulse focused onto the nanostructure, the tip will form plasma resonating with the external laser pulse, resulting in the spatial enhancement of the electric field. Driven by the enhanced electric field, gas-phase atoms will be ionized. The ionized electron density at different times can be obtained from the equation[33,34]

$$\frac{dN_\text{e}(t)}{dt} = W(t)\{N_\text{g} - N_\text{e}(t)\}, \tag{1}$$

where N_g is the initial Hydrogen gas density, and $W(t)$ is the instantaneous tunnel ionization rate.[35]

Once the electron is ionized at $t = t'$, it will be well controlled by the external fields, and the motion can be described classically by Newton's equation

$$\frac{d^2z}{dt^2} + E_\text{L}(z,t) = 0, \tag{2}$$

with an initial ionization position at $z = 0$. Here we assume that the electric field E_L only varies with space position z and time t for simplicity. From Eq. (2) we can obtain the classical trajectory of electrons, and through the derivation of position, we can also obtain the velocity at different times and positions. The collective motion of the electrons can form a directional current, which will be jointly contributed by the electrons ionized from time t_0 to t, i.e.,

$$J(t) = -\int_{t_0}^{t} v(t;t')dN_\text{e}(t'). \tag{3}$$

The intensity of THz emission is proportional to the derivative of this current,

$$E_\text{THz} \propto \frac{dJ(t)}{dt} = -\int_{t_0}^{t} E_\text{L}[z(t;t'),t]dN_\text{e}(t'). \tag{4}$$

Thus, by numerically solving the above equation, we can obtain the intensity of the radiation by Fourier transform of Eq. (4).

The quantum approach in this work is based on numerically solving the time-dependent Schrödinger equation (TDSE)[36–38] to double check the results. For atomic hydrogen interacting with a linearly polarized field ($E \parallel z$), the TDSE can be written as

$$i\frac{\partial}{\partial t}\psi(r,t) = \{\hat{H}_0(r) + \hat{V}(r,t)\}\psi(r,t), \tag{5}$$

where $\hat{H}_0(r)$ is the unperturbed Hamiltonian,

$$\hat{H}_0(r) = -\frac{1}{2}\frac{d^2}{dr^2} + \frac{\hat{L}^2}{2r^2} - \frac{1}{r}, \tag{6}$$

and $\hat{V}(r,t)$ is the potential for laser-atom interaction. The time propagation of the wave function can be obtained by the split-operator method as described in Refs. [36–38]. Once the time-dependent wave function is determined, the transient current can be written as

$$J(t) = -\frac{e}{m}\langle\psi(r,t)|\hat{p}|\psi(r,t)\rangle. \tag{7}$$

Then the radiation spectrum can be obtained from the Fourier transform of dJ/dt in Eq. (7).

Results and Discussion. In our simulations, a monochromatic laser pulse is assumed to be focused onto the tip of the nanostructure, the laser field is chosen to be a Gaussian form as $E(t) = E_\text{w}\exp[-2\ln 2\,(t^2/\tau^2)]$ with a duration $\tau = 5\,\text{fs}$. The reason for choosing an ultrashort pulse is as follows. Firstly, the damage threshold of the solid nanostructure is low in the long pulse. Secondly, the very short 5 fs pulse is asymmetric in the time domain, which is better for producing asymmetric drift current and efficient THz emission. Thirdly, the TDSE simulation is very time consuming when the laser pulse duration is long.

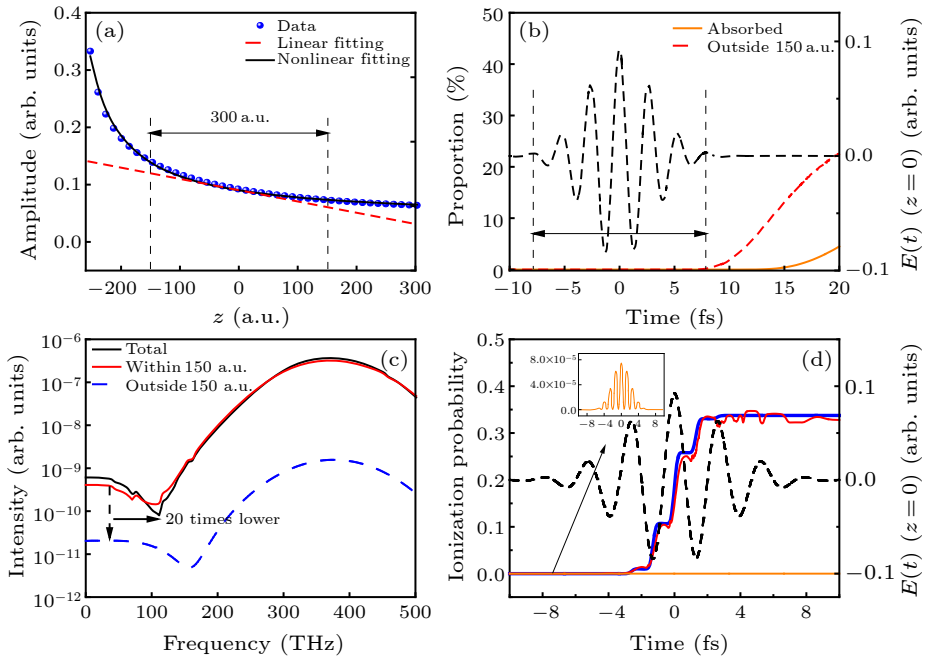

Fig. 2. (a) The induced electric field along the z axis. The simulation results by FDTD (blue dots) were fitted by nonlinear fitting (black line) and linear fitting (red line), respectively. (b) Proportions of electrons outside 150 a.u. (red dashed line) and absorbed at 300 a.u. (yellow solid line) during the laser pulse. (c) Radiation spectrum contributed by all electrons (black solid line), electrons within 150 a.u. (red solid line), and electrons outside 150 a.u. (blue solid line). (d) Ionization probability in the original input laser field (yellow solid line) and in the enhanced inhomogeneous laser field obtained from the quantum approach (red solid line). The blue solid line is the ionization probability obtained from Ref. [35].

In order to compare with the classical and quantum results, we set the gas density as $N_{\rm g} = 1.0$. Figure 2(a) shows the induced electric field versus the spatial position along the z axis at the tip of the nanostructure by FDTD. As we can see, with the increase of distance from the tip of nanostructure, the electric field shows a nonlinear downward trend, which can be well fitted by the formula

$$E_{\rm L}(z,t) = \Big(\frac{\alpha}{z+\beta} + \gamma\Big)E_0(t), \tag{8}$$

where α, β, and γ are the fitting parameters, and E_0 is the induced electric field strength $E(t)$ at $z = 0$. However, it is necessary to use the three parameters (in the simulation: $\alpha = 167.992$, $\beta = 306.956$, $\gamma = 0.428$) to describe the induced electric field distribution, which will make it difficult to analyze the generation of THz wave with the change of inhomogeneity. To simplify the fitting scheme required to characterize the induced field, we calculate the population of electrons within 150 a.u. and outside 150 a.u. during the laser pulse with the classical approach. Figure 2(b) shows the proportions of the electrons outside 150 a.u. and absorbed by the boundary. As we can see that during the laser pulse, only a small proportion of electrons will be driven to a far place where the electric field shows a great nonlinear trend. Most electrons do not travel very far from the position where they are ionized. Figure 2(c) presents the radiation spectrum contributed by the electrons within 150 a.u. and outside 150 a.u., respectively. Compared with the spectrum obtained from all electrons, the contribution of electrons outside the range of 150 a.u. is only a very small fraction. The yield contributed by the electrons within 150 a.u. is approximately at the same level as the intensity contributed by all electrons. It is about 20 times higher than that from electrons outside 150 a.u. This means that the dominant radiations is from the electrons within 150 a.u., in a relatively small range of space. Within this range, the change of electric field shows linear characteristics as illustrated in Fig. 2(a). Thus, it is more convenient for us to apply a linear fitting method:

$$E_{\rm L}(z,t) = (1 - gz)E_0(t), \tag{9}$$

which requires only one parameter g to characterize the inhomogeneity. The inhomogeneity is restricted to one dimension for simplicity because of the linearly polarized driving laser. However, this simplification has been proved to be effective in many studies as presented in the review of Ref. [15].

Based on the above analysis, the coefficient of inhomogeneity fitting is $g = 0.0021$. In addition, the inhomogeneity coefficient g varies with the angle θ of the triangular nanostructure. In our simulation, we take $\theta = 15°$, $g = 0.0046$; $\theta = 30°$, $g = 0.0021$; $\theta = 45°$, $g = 0.0015$. We can see that the amplitude of the electric field at $z = 0$ is about 10 times the amplitude of the input laser pulse. The effective intensity reaches $3 \times 10^{14}\,{\rm W/cm^2}$, which is about two orders of magnitude higher than the original intensity $3.9 \times 10^{12}\,{\rm W/cm^2}$. This leads to the increase in ionization rate, as shown in Fig. 2(d). This means that more electrons will be ionized to the continuum states, contributing to the generation of THz radiation. When the peak intensity of generated THz radiation is the same, we compare the laser intensity of the inhomogeneous field and the two-color field scheme. From Fig. 4(a), it can be seen that in

the range of 0–100 THz, the THz radiation generated by the inhomogeneous field ($g = 0.002$) is basically same as that generated by the two-color field, the intensity of the inhomogeneous and two-color field is 3.9×10^{12} W/cm^2 and 6.9×10^{15} W/cm^2, respectively, with about three orders of magnitude difference.

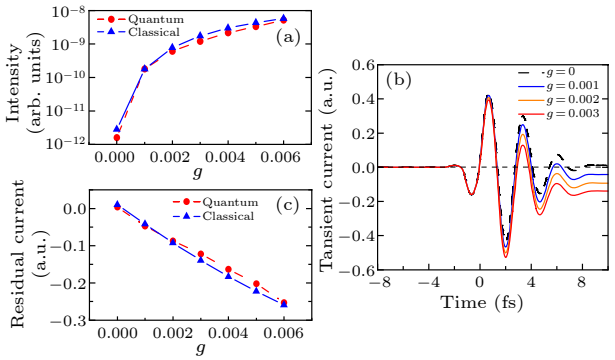

Fig. 3. (a) THz yield as a function of inhomogeneity g. (b) Evolution of the transient current with different g. (c) Residual current as a function of inhomogeneity g. In (a) and (c), the results from the quantum approach and the transient current model are compared.

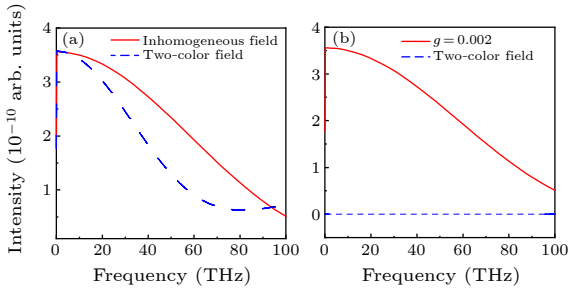

Fig. 4. (a) The intensity of generated THz radiation induced by inhomogeneous field scheme (3.9×10^{12} W/cm^2) and two-color field scheme (6.9×10^{15} W/cm^2). (b) The intensity of generated THz radiation induced by the same intensity (3.9×10^{12} W/cm^2) of the incident laser of inhomogeneous (solid line) and two-color field (dashed line).

To observe the effects on THz radiation with the change of inhomogeneity, we compute the radiation with different inhomogeneous coefficients g, but keeping the input driving laser intensity fixed. Figure 3(a) plots the yield of the radiation at 10 THz as a function of the inhomogeneous coefficient g obtained from both the transient current model and the quantum approach. As we can see, the results from both the approaches show a good agreement. Both of them demonstrate that with the increase of the spatial inhomogeneity of the field, the intensity of radiation in the THz range shows a great enhancement trend. In addition, when the intensity of incident laser is the same (3.9×10^{12} W/cm^2), we compare the THz radiation intensity induced by the inhomogeneous and two-color scheme. From Fig. 4(b), when $g = 0.002$, the peak intensity of THz radiation generated by the inhomogeneous field is far more than the two-color field, which indicates that the inhomogeneous field scheme needs modest incident laser intensity to generate THz radiation.

Since the enhancement of THz radiation has been observed, a question about the reason for the enhancement arises. First, we study the effects of spatial inhomogeneity on the transient current. Figure 3(b) shows the transient current with different inhomogeneities by TDSE. As we can see, there is nearly no directional current observed with $g = 0$. However, the transient current becomes more and more asymmetric as we increase the inhomogeneity g. This asymmetry leads to the generation of residual current after the laser pulse. Its Fourier transform will have a finite value at the zero frequency [11] as shown in Fig. 2(c). Figure 3(c) plots the residual current as a function of inhomogeneous coefficient g. As we can see, when we increase the spatial inhomogeneity, the amplitude of the residual current shows an increasing trend. The residual current from the classical model has also been plotted. The discrepancy is very small, which may come from the neglect of atomic potentials, transport, and re-scattering effect in the transient current model. The trends are approximately the same. Just as the intensity of THz radiation increases with the change of spatial inhomogeneity, the residual current shows the same trend with THz radiation. It reminds us that there might be a relation between the transient current and the intensity of THz radiation. According to the transient current model, THz radiation is proportional to the derivative of transient current $J(t)$, thus the intensity of radiation at frequency Ω from Fourier transform can be written as

$$I(\Omega) = \left|\frac{1}{T}\int_0^T \frac{dJ(t)}{dt} e^{-i\Omega t} dt\right|^2, \tag{10}$$

where T is the duration of the laser pulse. Considering that we are interested in the THz range, Ω is much smaller than the frequency of the laser used here. However, the period of THz wave is much larger than the duration of the laser pulse T, which means that the change of $e^{-i\Omega_{\rm THz}t}$ is very small in the integral from 0 to T. This term can be neglected, thus we can rewrite Eq. (10) as

$$I(\Omega_{\rm THz}) \propto \left|\int_0^T \frac{dJ(t)}{dt} dt\right|^2, \tag{11}$$

where $e^{-i\Omega_{\rm THz}t}$ is approximately 1. From Eq. (11), we can obtain

$$I(\Omega_{\rm THz}) \propto \left|J(T) - J(0)\right|^2 = \left|J(T)\right|^2. \tag{12}$$

The intensity of THz radiation is proportional to the square of the final residual current $J(T)$. This implies that the radiation at THz range is strongly associated with the final residual current. The spatial inhomogeneity causes the asymmetry of the transient current, then the asymmetry of the current leads to the increase of the residual current and the enhancement of THz radiation. Although this scheme is different from the two-color field scheme, [39,40] they all produce the drift current and efficient THz emission.

Considering that the transient current is contributed by the electrons moving in the inhomogeneous field, it is necessary to analyze electrons' dynamic process driven by the induced field. Figure 5(a) shows the time evolution of electrons' classical trajectories in electric fields with different spatial inhomogeneities. As we can see, the spatial inhomogeneity of the electric field leads to the asymmetric

electrons motion, and causes the electrons to move away from the tip of the nanostructure, where the induced electric field is weaker. As a result of this asymmetric movement, electrons can obtain more velocities away from the tip, leading to the asymmetry of electrons' velocity as illustrated in Fig. 5(b). The asymmetry is more obvious as we increase the spatial inhomogeneity.

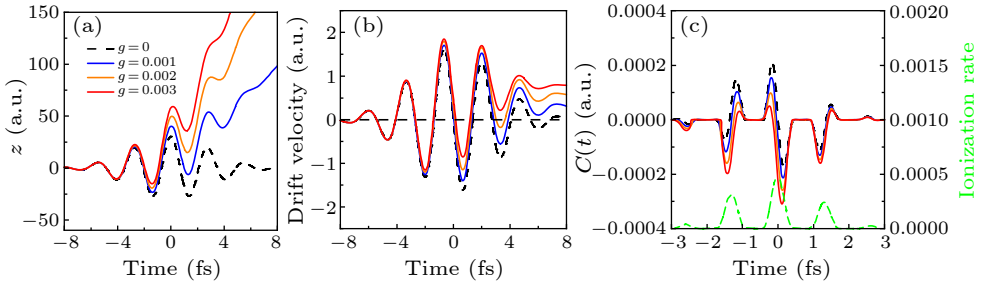

Fig. 5. [(a), (b)] Evolution of electrons classical trajectories and velocities with different inhomogeneous coefficients. The initial position and velocity are chosen to be $z = 0$ and $v = 0$, respectively. (c) Contributions of electrons $C(t)$ ionized at different times to the residual current. The green dashed line represents the ionization rate.

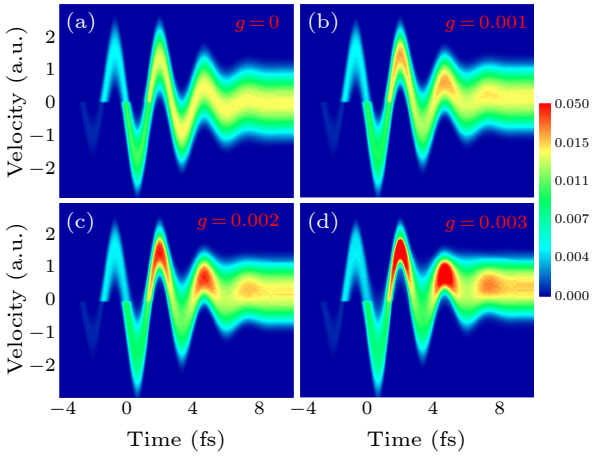

Fig. 6. Variation of electrons' population at different velocities over time for different spatial inhomogeneity g.

To observe the motion of all the ionized electrons, we also compute the population of electrons at different velocities during the laser pulse as depicted in Fig. 6. As we can see, in homogeneous fields, the population of electrons at the velocity towards the tip (negative) and away from the tip (positive) are symmetric as shown in Fig. 6(a), which causes the transient current formed by them to cancel each other, resulting in zero residual current arising in the process. However, with the increase of the spatial inhomogeneity of the electric field, more electrons can acquire the velocity away from the tip as shown in Figs. 6(b) and 6(c). This leads to the asymmetry of electrons' population at different velocities, and the transient current towards the tip formed by the electrons will become dominant, resulting in the generation of non-vanishing residual currents.

Meanwhile, in order to see the contribution of electrons ionized at different times to the residual current, we also plot the components of residual current contributed by electrons ionized at different times as illustrated in Fig. 5(c). As we increase the inhomogeneity, more electrons ionized from different times will finally incline to form a residual current towards the tip (negative direction). This tendency is more obvious as the spatial inhomogeneity is stronger. Another result we can obtain from the figure is that the residual current is mainly contributed by the electrons ionized at the peak of the laser pulse, since more electrons will be ionized at the peak amplitude of the laser pulse.

In conclusion, we have theoretically investigated the THz emission mechanism of gas atoms in a local inhomogeneous field induced by triangular metallic nanostructures irradiated by an ultrashort laser pulse. Compared to the intense two-color asymmetric laser fields reported previously, the advantage of this scheme is that the input laser field is monochromatic and the intensity is rather low. The experimental realization is much easier. The simulation results show that such triangular nanostructures are capable of providing us with an enhanced and spatially asymmetric field to enable the enhancement of THz radiation. We expect that our work can inspire further research of THz generation by means of other optimized nanostructures.

Acknowledgement. This work was supported by the National Natural Science Foundation of China (Grants Nos. 12174090 and 12074105), the Science and Technology Project of Henan Province (Grant No. 22210210176), and the Cooperative Project of Henan Normal University with Fuhuide Trade Co., Ltd of Henan Province (Grant No. XH2019005).

References

[1] E Y W, Zhang L, Tcypkin A, Kozlov S, Zhang C, and Zhang X C 2021 *Ultrafast Sci.* **2021** 9892763
[2] Zhang Z L, Zhang J Y, Chen Y P *et al.* 2022 *Ultrafast Sci.* **2022** 9870325
[3] Song B Q and Yang X *et al.* 2023 *Ultrafast Sci.* **3** 0007
[4] Du H C, Wang H Q, and Hu B T 2011 *Chin. Phys. B* **20** 044207
[5] Yuan K J and Bandrauk A D 2013 *Phys. Rev. Lett.* **110** 023003
[6] Zhao T and Wu Z H 2020 *Chin. Phys. B* **29** 034101
[7] Yeh K L, Hoffmann M C, Hebling J, and Nelson K A 2007 *Appl. Phys. Lett.* **90** 171121
[8] Kim K Y, Glownia J H, Taylor A J, and Rodriguez G 2007 *Opt. Express* **15** 4577
[9] Xie X, Dai J, and Zhang X C 2006 *Phys. Rev. Lett.* **96** 075005

[10] Kim K Y, Glownia J H, Taylor A J, and Rodriguez G 2012 *IEEE J. Quantum Electron.* **48** 797
[11] Zhang L, Wang G L, and Zhou X X 2016 *J. Mod. Opt.* **63** 2159
[12] Du L L, Zhao S F, Zhou X X, and Zhao Z X 2015 *Chin. Phys. B* **24** 043203
[13] Xu X, Huang Y D, Zhang Z L *et al.* 2023 *Chin. Phys. Lett.* **40** 045201
[14] Kim K Y 2009 *Phys. Plasmas* **16** 056706
[15] Ciappina M F 2017 *Rep. Prag. Phys.* **80** 054401
[16] Kim S, Jeong T I, Park J, Ciappina M F, and Kim S 2022 *Nanophotonics* **11** 2393
[17] Kim S, Jin J, Kim Y J, Park I Y, Kim Y, and SW K 2008 *Nature* **453** 757
[18] Xue S, Du H C, Xia Y, and Hu B T 2015 *Chin. Phys. B* **24** 054210
[19] Zhang J 2016 *Laser Phys. Lett.* **13** 075302
[20] Ciappina M F, Acimovic S S, Sharan T, Biegert J, Quidant R, and Lewenstein M 2012 *Opt. Express* **20** 26261
[21] Feng L Q 2015 *Phys. Rev. A* **92** 053832
[22] MF C, Biegert J, Quidant R, and Lewenstein M 2012 *Phys. Rev. A* **85** 033828
[23] Wang Z, He L, Luo J, Lan P, and Lu P 2014 *Opt. Express* **22** 25909
[24] Zhao J and Zhao Z X 2010 *Chin. Phys. Lett.* **27** 063301
[25] Herink G, DR S, Gulde M, and Ropers C 2012 *Nature* **483** 190
[26] Krüger M, Schenk M, and Hommelhoff P 2011 *Nature* **475** 78
[27] Ropers C, Solli D R, Schulz C P, Lienau C, and Elsaesser T 2007 *Phys. Rev. Lett.* **98** 043907
[28] Piglosiewicz B, Schmidt S, Park D J *et al.* 2014 *Nat. Photon.* **8** 37
[29] Zhang H D, Liu X W, Jin F C *et al.* 2021 *Chin. Phys. Lett.* **38** 063201
[30] Zhong H Y, Guo J, Feng W, Li P C, and Liu X S 2016 *Phys. Lett. A* **380** 188
[31] Corkum P B 1993 *Phys. Rev. Lett.* **71** 1994
[32] Oubre C and Nordlander P 2005 *J. Phys. Chem. B* **109** 10042
[33] de Alaiza Martínez P G, Babushkin I, Bergé L *et al.* 2015 *Phys. Rev. Lett.* **114** 183901
[34] Babushkin I, Skupin S, Husakou A *et al.* 2011 *New. J. Phys.* **13** 123029
[35] Wu H C, Meyer-ter-Vehn J, and Sheng Z M 2008 *New. J. Phys.* **10** 043001
[36] Zeng S L, Zou S Y, and Yan J 2009 *Chin. Phys. Lett.* **26** 053202
[37] Chu S I and Tong X M 1998 *Chem. Phys. Lett.* **294** 31
[38] Tong X M and Chu S I 1997 *Chem. Phys.* **217** 119
[39] Wang W M, Sheng Z M, Wu H C *et al.* 2008 *Opt. Express* **16** 16999
[40] Zhang L L, Wang W M, Wu T *et al.* 2017 *Phys. Rev. Lett.* **199** 235001